UCLA-12-8 72

UNIVERSITY OF CALIFORNIA, LOS ANGELES

LABORATORY OF NUCLEAR MEDICINE AND RADIATION BIOLOGY

CONTRACT NO. AT (04-1) GEN-12

A CRITICAL EVALUATION OF POTASSIUM-43 AND CESIUM-129 FOR QUANTITATIVE MYOCARDIAL SCANNING*

N.D. Poe, L.M. Eber, L.S. Graham, W. Nikesch, and N.S. MacDonald
The Laboratory of Nuclear Medicine and Radiation Biology,
and the Departments of Radiological Sciences and Medicine,
School of Medicine, University of California,
Los Angeles, California, USA

Mailing Address:

Norman D. Poe, M.D.
Laboratory of Nuclear Medicine
900 Veteran Ave.
Los Angeles, California 90024
USA

* This work was supported by AEC Contract AT(04-1) GEN-12 between the U.S. Atomic Energy Commission and the University of California and Contract No. NIH-71-2491 under the Myocardial Infarction Program, National Heart and Lung Institute, NIH, Department HEW.

A CRITICAL EVALUATION OF POTASSIUM-43 AND CESIUM-129 FOR QUANTITATIVE MYOCARDIAL SCANNING

N.D. Poe, L.M. Eber, L.S. Graham, W. Nikesch, and N.S. MacDonald
The Laboratory of Nuclear Medicine and Radiation Biology,
and the Departments of Radiological Sciences and Medicine,
Center for Health Sciences, University of California,
Los Angeles, California, USA

The recent availability of potassium-43 and cesium-129 has revived interest in myocardial scanning. This study was undertaken to compare imaging characteristics of these two ions for the purpose of quantitating myocardial infarction. Both nuclides were produced on-site in a small biomedical cyclotron.

Instrumentation: Although better quality images could be obtained with rectilinear scanners, emphasis was placed on scintillation camera imaging because of ease of quantitation. A high efficiency pinhole collimator proved most satisfactory. Modulation transfer functions showed poorer resolution with potassium-43 due to collimator penetration from the .619 MEV photons.

Animal Experiments: After intravenous injections in dogs, between 5-8% of the administered dose concentrated in myocardium. Potassium reached peak values in 10-20 minutes, then cleared rapidly ($T\frac{1}{2}$ 6 hours). Cesium turnover was slower with a peak between 1-3 hours and a $T\frac{1}{2}$ approaching one day. Myocardial extraction efficiency, determined by direct intracoronary injection, was 70% for potassium, 20% for cesium. Acute and chronic ischemia and/or infarction were produced by ligation of the anterior descending coronary artery at different levels. Small lesions were not detected in vivo and even large lesions were often not clearly enough defined for quantitation.

Clinical Investigations: Correlative studies were performed in patients undergoing cardiac catheterization and ventriculography. With nuclide doses up to 2.5 mCi by intravenous injection and 1.0 mCi by intracoronary injection, satisfactory anterior and right and left anterior

oblique views are obtainable. The anterior image is "O" or "U" shaped and represents left ventricular and septal muscle mass with a central ventricular cavity defect. There is also a tendency for diminished apical activity. These factors combine to obscure anterior and apical lesions. Resolution is further reduced by a low 4:1 target-to-background ratio after intravenous injections. The ratio can be increased to 7:1 with cesium by intracoronary injection. Although the myocardial extraction of potassium is more efficient and gives higher ratios, this advantage is quickly lost by its more rapid clearance.

In over 30 patients studied by intravenous and/or intracoronary injections of cesium-129 and potassium-43, only large abnormalities such as aneurysms could be defined consistently. It is concluded that radiopharmaceuticals with greater myocardial specificity are needed for quantitative measurement of regional myocardial ischemia.

INTRODUCTION

The widespread incidence of coronary artery disease has stimulated interest in noninvasive techniques to evaluate the extent and severity of the disease process. Specifically, there is a need to localize the sites of injury and to quantitate the degree of ischemia. External detection of gamma-emitting radionuclides as they pass through the coronary vessels and/or localize in the myocardium is a logical approach to this problem. More precise anatomic localization of abnormalities would be possible with the addition of scintiscanning. This concept is not new and a number of radiopharmaceuticals for myocardial scanning have been investigated [1]. The most promising agents were potassium and its analogs, rubidium and cesium, but imaging with the available nuclides was unsatisfactory because the energies were either too high or too low. In the past few years, potassium-43 and cesium-129 have become available. Both of these radionuclides have energies which are suitable for imaging by either scintillation cameras or rectilinear scanners [2,3].

The purpose of this study is to further define the turnover characteristics of potassium and cesium in normal and ischemic myocardium and to determine the usefulness of ^{43}K and ^{129}Cs in the clinical evaluation of coronary artery disease.

RADIONUCLIDE PRODUCTION

Both ^{43}K and ^{129}Cs are produced on-site in a small biomedical cyclotron.[1] (^{42}K and ^{131}Cs, used in some animal experiments, were obtained from commercial sources.) The potassium is made by the ^{40}Ar (α,p) ^{43}K reaction from bombardment of purified argon gas with 20.4 MEV alpha particles in a gold-plated brass cylinder. The resultant pure ^{43}K is rinsed out with normal saline. The average yield at the end of bombardment is 0.08 mCi per μA-hour. The typical usable yield 100 minutes after a 2 hour run is about 2.5 mCi. Attempts are being made to increase this yield.

^{129}Cs is made by 24.6 MEV alpha bombardment of sodium iodide by the ^{127}I $(\alpha,2n)^{129}Cs$ reaction. The product is dissolved in pyrogen-free distilled water sufficient to make the final solution isotonic. Small amounts of ^{22}Na are present. The average yield is 0.15 mCi per μA-hour. The typical usable yield is 5 mCi 16 hours after a 2 hour bombardment. A delay of 12-16 hours is required for decay of ^{130}Cs arising from the (α,n) reaction.

INSTRUMENTATION

The selection of instrumentation was based on observations with ^{129}Cs, the first analog available to us. It was generally agreed that the best quality in vivo images were obtained in both animals and humans with a 3-inch rectilinear scanner using a medium energy collimator. However, for speed and potential ease of regional quantitation, a large crystal scintillation camera[2] was chosen. As images obtainable with a straight bore collimator were small and failed to optimally utilize the available

---

[1] Cyclotron Corporation, Berkeley, California.

[2] Picker Dynacamera 2B.

crystal surface, a converging collimator was tried. The distortion with this collimator at all distances was so great as to produce a totally useless image. A pinhole collimator with a high sensitivity aperture of slightly over 80 mm was finally selected. For most anterior studies, the collimator was positioned 6 cm from the chest wall. This distance provided an axial magnification factor of approximately 2. Although greater magnification would be desirable, distortion of the three dimensional myocardial image became excessive if closer positioning was attempted.

^{43}K and ^{129}Cs have dominant gamma emissions similar to ^{131}I. However, ^{43}K has a significant high energy contribution which possibly could lead to loss of resolution. The major gamma energies (MEV) and intensities for ^{43}K are 0.373(85%), 0.390(18%), 0.590(13%), 0.619(81%); and for ^{129}Cs are 0.375(48%), 0.416(25%), 0.550(5%). It was our opinion that slightly better images were obtainable with ^{129}Cs (Fig. 1). In an attempt to clarify this point, the two radionuclides were compared by determining modulation transfer functions and penetration fractions. The MTF's for 90 cm line sources at a distance of 10 cm from the collimator are seen in Figure 2. The curves are very close, suggesting only a slight superiority for ^{129}Cs. However, using the same line sources, the penetration fraction for ^{129}Cs is 0.14 in contrast to a fraction of 0.61 for ^{43}K. The lateral penetration of ^{43}K photons from nontarget sources, particularly after total body distribution following intravenous administration, could noticeably degrade the resultant scan image.

ION KINETICS

Normal potassium and cesium uptake and turnover characteristics were determined in anesthetized dogs [4]. Average values following intravenous injections are found in Figure 3. Blood clearance for both ions is multiphasic, but is more rapid and complete for potassium. Precordial uptake of potassium reaches a peak within 20 minutes after injection, then begins an immediate decline with a half-time of approximately 6 hours. The peak for cesium is gradually achieved between 1-3 hours followed by a slow and prolonged clearance estimated to be about 24 hours. The precordial curve is only an approximation of myocardial concentration as both blood clearance and overlying skeletal muscle uptake are reflected. Similarly, the head curve is a combination of blood clearance and skeletal muscle uptake. In Figure 3, note the flatness of the head curves which demonstrates the concentration and slow turnover of these ions in skeletal muscle. The relatively low myocardial concentration of potassium and cesium (5-8% of the injected dose) plus substantial uptake in overlying tissue result in a low target-to-background ratio which poses a problem in the use of these ions for quantitative investigations. The high background is maintained because renal clearance of these ions from the total body potassium pool is very slow.

Myocardial extraction efficiency was determined in anesthetized open-chest dogs by myocardial counting following direct intracoronary injection of ^{42}K and ^{131}Cs. About 70% of the administered potassium is retained during the first circulation. The clearance $T\frac{1}{2}$ by this route is slightly over 1 hour. With injected cesium, only 20% is retained on the first passage and the clearance $T\frac{1}{2}$ is 6 hours.

Acute and chronic (up to 6 months) ischemic lesions and infarcts were produced in 30 open-chest dogs by single or multiple ligations of the anterior descending coronary artery and major tributaries. At selected intervals, technetium-99m labeled resin microspheres (<35μ diameter) and ^{131}Cs or ^{129}Cs were simultaneously injected into the left atrium. Thirty minutes later, the animal was sacrificed and multiple sections of the myocardium were counted in a dual spectrometer well-counter. The relative counts of the two radionuclides correlated closely and showed decreased concentration in the ischemic areas. The attained level of activity was assumed to represent relative blood flow. However, if cesium is given intravenously and incorporated into the myocardium prior to vascular occlusion, there is a definite lag time before cesium is lost from the damaged cells. Even in severely injured tissue, insignificant amounts are cleared in the first 6 hours. By 24 hours considerable cesium is lost but the amount retained is approximately two times the amount taken up after post-occlusion injection. In other words, equilibration between loss from injured or dead cells and blood flow is not yet attained by 24 hours. Similar studies with preinfarction administration of potassium were not performed, but Jennings et al. [5] have previously studied this problem. Their results indicate that clearance from dead cells and equilibration with blood flow are more rapid with potassium than cesium.

DOSIMETRY

The human dosimetry calculations were derived from MIRD Committee sources (Supplement 4, Pamphlet 6 for ^{43}K, and prepublication data for ^{129}Cs) and from the animal turnover data above. The following assumptions were used for both radionuclides: 1.0 mCi intravenous dose, 5% myocardial uptake, 300 gm heart mass, and no total body clearance. For ^{43}K the biologic half-time in the heart was 6 hours; and for ^{129}Cs the biologic half-time was equated with the physical half-time. These assumptions presumably tend to overestimate the actual dosage delivered. ^{43}K gives 1.24 rads to the myocardium and 0.59 rads to the total body. Corresponding ^{129}Cs values are 1.05 rads and 0.22 rads. With direct intracoronary arterial injection, the myocardial dose for both radionuclides would increase significantly, but the total body dose would decrease only slightly because the ions which are rapidly cleared from the myocardium would quickly enter the total body potassium pool with radiation effects similar to those found after intravenous injection.

To date, UCLA Human Use Committee approval has been granted only to study patients with heart disease undergoing cardiac catheterization. For both nuclides, intravenous doses up to 2.5 mCi can be given and intracoronary doses up to 1.0 mCi. Under optimal conditions, these doses provide between 50,000 and 100,000 counts in ten minutes or less. The ten minute time interval was arbitrarily selected as a period suitable for utilization of this type of procedure in acutely ill patients or as a screening test.

IMAGING OF EXPERIMENTAL INFARCTION

The de novo detection of ischemic defects following coronary artery ligation has proven to be a definite problem. Scans obtained from normal animals in the anterior and left lateral projections show so much variation

that it is often impossible to differentiate ischemic lesions from areas which normally contain relatively low levels of activity. In the anterior projection, there is a centrally located region of diminished uptake which represents the left ventricular cavity. Also, in most animals, there is a less well defined decrease in activity at the apex (Fig. 1). In the left lateral view, an irregular band-like region of relatively low radionuclide content extends from the apex to the base (Figs. 1, 4A, 5A). The exact etiology of this defect is not yet ascertained but presumably represents a combination of the ventricular and apical variations noted in the anterior projection.

With reference to Figures 4B and 5B, there is no problem in identifying the anterior defects in the postinfarction scans as abnormalities. However, in Figure 1, the possibility of an apical lesion in the baseline scan cannot be excluded. A similar statement could be made for the baseline scan in Figure 4.

Although precise determinations of the size of defects that can be indisputably detected by scanning have not yet been established, it is apparent that only large lesions involving most of the anterior surface of the heart can be consistently detected in vivo. Even with baseline reference scans and electrocardiographic evidence of acute infarction, many infarcts go undetected. This failure occurs inspite of relative reductions in radionuclide concentration in the infarct of 80% or more as determined by in vitro counting.

Once an abnormality is detected, there is no way of differentiating acute damage from healed scar tissue. In ischemic tissue, the concentration of the tracer closely correlates with the relative blood flow. After infarction, the radionuclide content of the dead tissue comes into equilibrium with the extracellular fluid. With healing the infarcted muscle is replaced with fibrous tissue. The cells in the scar also take up the tracer but the concentration on a per gram basis is about one-half or less the concentration in the surrounding myocardium. The low potassium or cesium content, the relative thinness of the healed infarct plus a tendency for hypertrophy of the adjacent myocardium all combine to enhance the probability of detecting old infarcts.

Reduced blood flow without tissue injury or infarction is not detectable with static imaging. Simple ligation of the anterior descending coronary artery often produces no scan or electrocardiographic evidence of ischemia. Obviously, collateral flow can be sufficient to prevent cellular damage but absolute flow is almost certainly reduced initially. From this observation, it is probable that stenotic lesions, even of high degree, will not produce scan abnormalities.

As will be seen below, the problems encountered in detecting experimental ischemia and infarction in dogs apply equally to clinical investigations.

CLINICAL INVESTIGATIONS

The basic purpose of our investigation is to develop a simple, rapid intravenous scintiscan technique for detecting and quantitating regional myocardial injury, ischemia, and infarction. The investigational plan was to perform correlative scan studies in coronary artery disease patients undergoing cardiac catheterization, coronary angiography, and ventriculography. Scans after intravenous administration of tracer were to be

obtained the day before or after catheterization. Comparative images made after selective intra-arterial injection during the catheterization procedure were also to be obtained. This approach was not followed closely for two reasons. First, the target-to-background ratios available after intravenous injection of either ^{129}Cs or ^{43}K give such poor quality scans that quantitative and even qualitative estimates of regional perfusion are difficult (Figs. 6, 7). Second, the slow myocardial clearance of cesium makes repeat studies within 24 hours almost impossible. It is anticipated that computer manipulation of the data, not available at the time of writing, will be required to solve these problems and to eventually determine the practicality and usefulness of the intravenous route. As a result of those limitations, most of the patients studied have had either intravenous or intracoronary administration of radionuclide, not both.

The selection of positions for which to view the myocardium are dictated by both practical and theoretical considerations. For comparison with electrocardiographic and special radiographic data, the anterior and right and left anterior oblique positions (camera positioned anteriorly to the patient) are best. These views are easily and most satisfactorily obtained. The straight left lateral projection is more difficult because of greater target distance and a tendency for superimposition on the liver. With a standard scintillation camera, the posterior projection is essentially unobtainable because of the interposed skeletal muscle barrier which contains high concentrations of injected radionuclide. Failure to obtain these two views is a major disadvantage because it precludes evaluation of the inferior and posterior walls of the heart. Unfortunately, the anterior and oblique projections also have other limitations which will be described below.

Although over 30 patients have been studied, the high incidence of myocardial disease has interfered with establishment of normal image patterns. Based on a few left coronary injections in subjects with nonsclerotic dominant left coronary arteries (Figs. 6C, 8), the normal anterior projection shows an ellipsoidal image, primarily representing the left ventricular muscle mass. The blood filled left ventricular cavity is seen variably as a central defect. There is a tendency for decreased activity at the apex. The left anterior oblique image is rounder and the central and apical defects are more prominent. In the right anterior oblique, the central defect is less noticeable and the anterior surface is rounded. In diseased hearts, the anterior image assumes a more circular shape and the central defect in the anterior and left oblique images becomes more evident.

As was seen with the dog work, distinguishing true abnormalities from normal variations in activity in the ventricular cavity and the apex becomes a serious problem in all but the most extensive lesions. For example, in Figure 9, the large apical and free wall defect is easily seen in a patient who has a massive ventricular aneurysm demonstrated by akinesis on the corresponding ventriculogram. In contrast, compare the two examples in Figure 8. The relative images are reasonably similar. The potassium patient has no demonstrable arterial disease by angiography, but the cesium patient has extensive disease consisting of right coronary artery occlusion with collateral reconstitution, 80% stenosis of the anterior descending coronary artery, partial circumflex involvement, and apical akinesis from an old inferior myocardial infarction. Although the cesium scan series would not be interpreted as normal, the extent and severity of the disease is simply not evident.

An interesting question arises from the foregoing example. Would potassium have been more sensitive than cesium in demonstrating the pathology? There is some experimental evidence to suggest it could have. Love et al. [6] have shown a relatively constant myocardial extraction of cesium independent of flow but potassium extraction increases as flow increases. These findings combined with the more rapid blood clearance of potassium could be expected to provide greater contrast between well perfused and poorly perfused regions. Further studies will be required to clarify this point, but the exchange kinetics of these two analogs differ sufficiently to postulate that significant differences could exist in the distribution patterns found in conditions of altered perfusion.

COMMENTS

Although the general tenor of this paper casts doubt on the reliability of quantitative myocardial imaging with potassium analogs, considerably more basic and clinical investigative work is necessary before a final decision is reached. Immediate improvement in results can be anticipated with computerized data manipulation. Heart motion can be reduced and the target-to-background ratio can be improved. Dynamic imaging of multiple regions-of-interest may be of value. Normal distribution patterns and probability estimates of abnormality can be determined. The computer can also be of value for storing, adding, and subtracting data collected after selective serial injections of the coronary arteries with ^{43}K. Improved resolution and sensitivity in the instrumentation will also help improve the results.

Nevertheless, for practical application, the real need is for new radiopharmaceuticals with greater myocardial specificity. Only by this means will quantiative imaging after intravenous administration become practical. It is probable that several agents which behave differently in ischemic, infarcted, and scarred tissue will be necessary for complete characterization of the abnormalities occurring in coronary artery disease.

REFERENCES

1. ZARET, B.L., PITT, B., and ROSS, R.S., Determination of the Site, Extent, and Significance of Regional Ventricular Dysfunction during Acute Myocardial Infarction. Circ. 45:441-456, 1972.
2. HURLEY, P.J., et al., ^{43}KCl: A New Radiopharmaceutical for Imaging the Heart. J. Nucl. Med. 12:516-519, 1971.
3. YANO, Y., et al., Myocardial Uptake Studies with ^{129}Cs and the Scintillation Camera. J. Nucl. Med. 11:663-668, 1970.
4. POE, N.D., Comparative Myocardial Uptake and Clearance Characteristics of Potassium and Cesium. J. Nucl. Med. 13:557-560, 1972.
5. JENNINGS, R.B., CROUT, J.R., and SMETTERS, G.W., Studies on Distribution and Localization of Potassium in Early Myocardial Ischemic Injury. Arch. Pathol. 63:586-592, 1957.
6. LOVE, W.D., et al., Differences in the Relationships between Coronary Blood Flow and Myocardial Clearance of Isotopes of Potassium, Rubidium and Cesium. Am. Heart J. 76:353-355, 1968.

LEGENDS

Figure 1: Comparison of images obtained with ^{129}Cs and ^{43}K using a 3-inch rectilinear scanner and a large crystal scintillation camera. In general, scans performed on a rectilinear scanner using ^{129}Cs give the best resolution. With the camera, cesium also shows better detail, but physiologically may not provide as reliable information as does potassium. (Arrows indicate apex.)

Figure 2: Modulation transfer functions for ^{129}Cs and ^{43}K from a large crystal scintillation camera equipped with a high sensitivity pinhole collimator. The MTF's were obtained from a 90 cm line source covered by 2.5 cm of lucite and placed 10 cm from the collimator.

Figure 3: Clearance curves for potassium (A) and cesium (B). The turnover characteristics of these two ions are distinctly different with potassium showing more rapid uptake and clearance. (Count rates adjusted for graphic purposes.)

Figure 4: Baseline (A) and immediate postinfarction (B) left lateral scans and lead AVL electrocardiographic tracings in a dog following ligation of the anterior descending coronary artery. Note the development of a large anterior scan defect and ECG evidence of acute infarction in the follow-up study.

Figure 5: Baseline (A) and 6 month postinfarction (B) left lateral scans and lead AVF electrocardiographic tracings in a dog following ligation of the anterior descending coronary artery. A distinct anterior defect developed after infarction. The follow-up ECG shows only ischemia.

Figure 6: Relative target-to-background ratios with ^{129}Cs and ^{43}K by different injection routes. (A) intravenous cesium, (B) intravenous potassium, (C) intracoronary cesium, (D) intracoronary potassium. Similar ratios are found in the intravenous studies, but far superior values can be obtained with intracoronary potassium.

Figure 7: Anterior and left and right anterior oblique scans following intravenous injection of ^{129}Cs in a patient with a dilated, thin myocardium. This is an example of the best quality image obtained by this injection route.

Figure 8: Intracoronary arterial injections. The patient receiving ^{43}K has no demonstrable coronary artery disease by angiography. The ^{129}Cs patient has severe triple vessel disease and an old apical infarction. The extent of the disease in the second patient is not evident from these studies.

Figure 9: Anterior and right anterior oblique images after left coronary arterial injection of ^{129}Cs. A large apical defect supports a diagnosis of left ventricular aneurysm. The ventriculogram shows little evidence of ventricular contraction from diastole (solid line) to systole (dotted line).

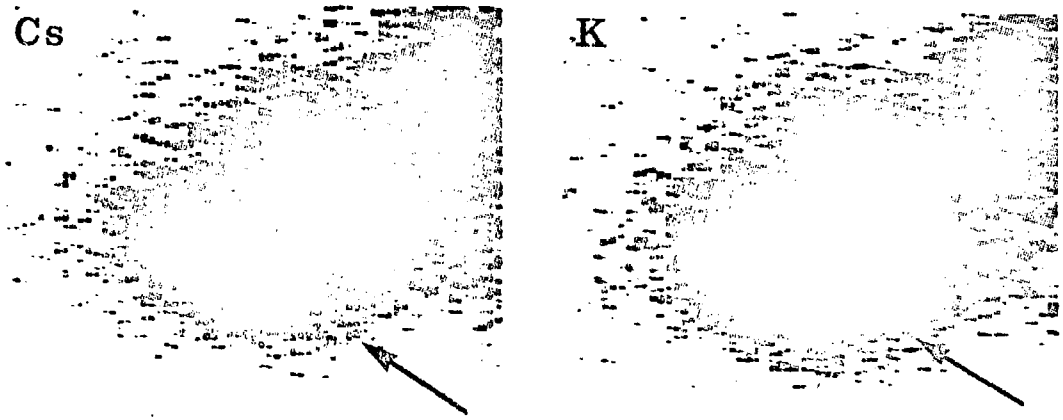

RECTILINEAR (LEFT LATERAL)

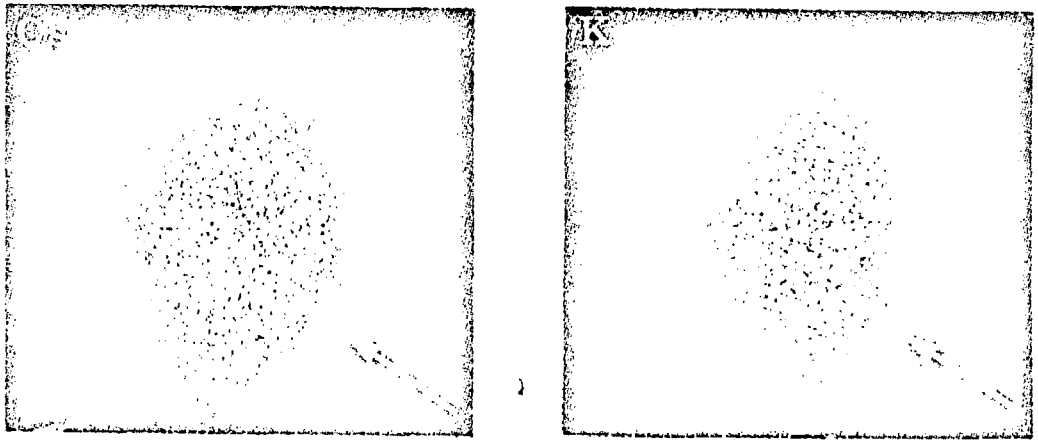

CAMERA (ANTERIOR)

FIGURE 1.

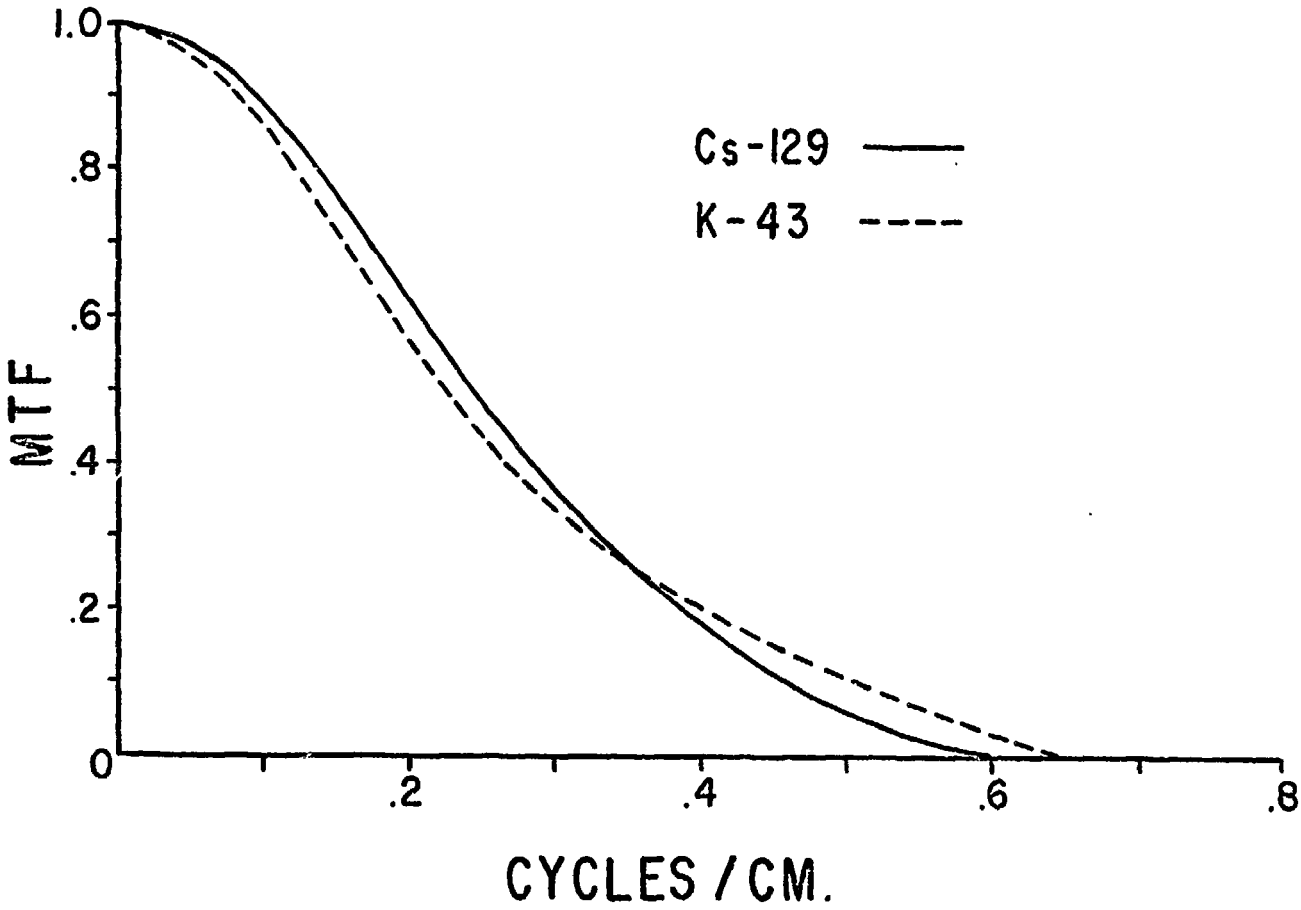

FIGURE 2.

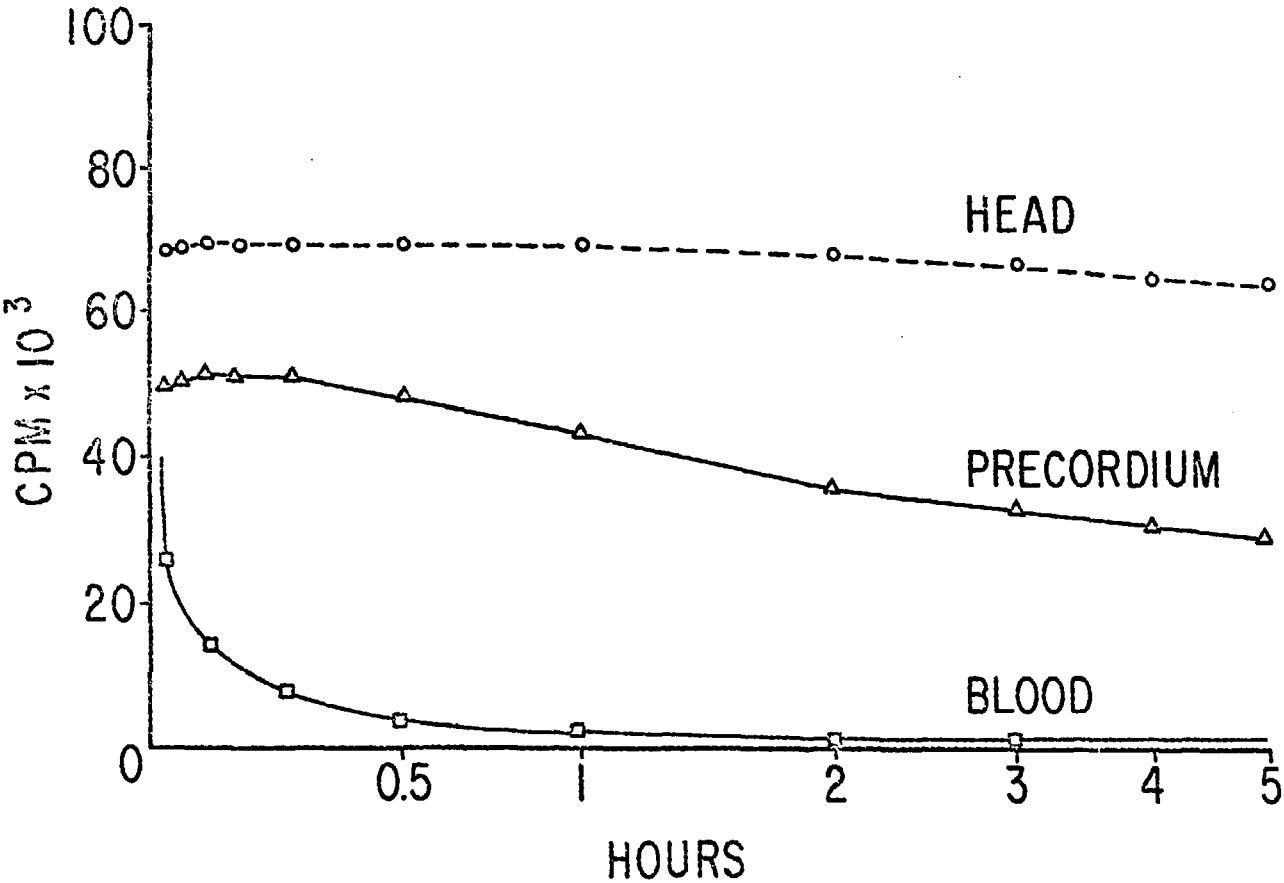
100
80
60
40
20
0
CPM x 10³
HEAD
PRECORDIUM
BLOOD
0.5
1
2
3
4
5
HOURS

FIGURE 3A.

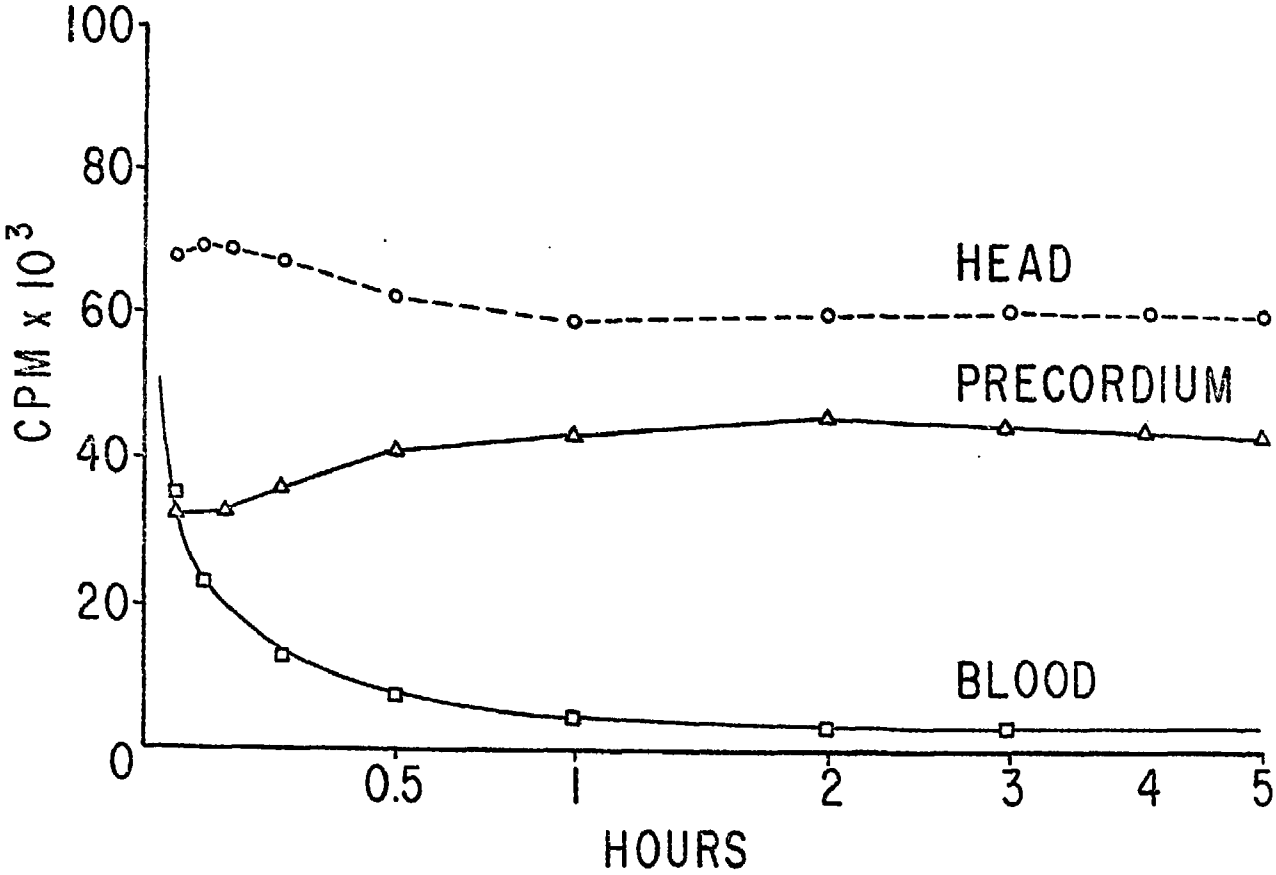
100
80
60
40
20
0
CPM x 10^3
HEAD
PRECORDIUM
BLOOD
0.5
1
2
3
4
5
HOURS

FIGURE 3B.

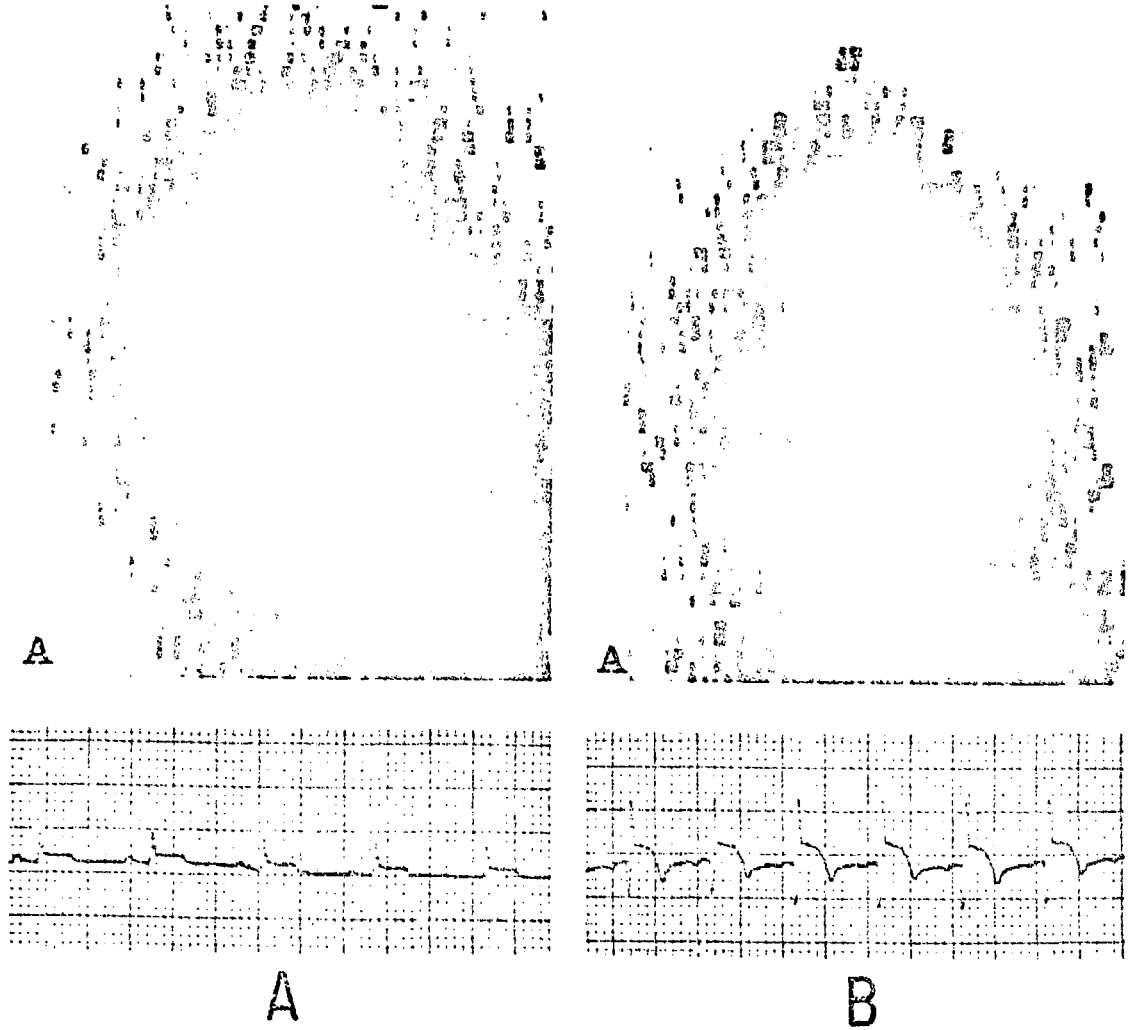

FIGURE 4.

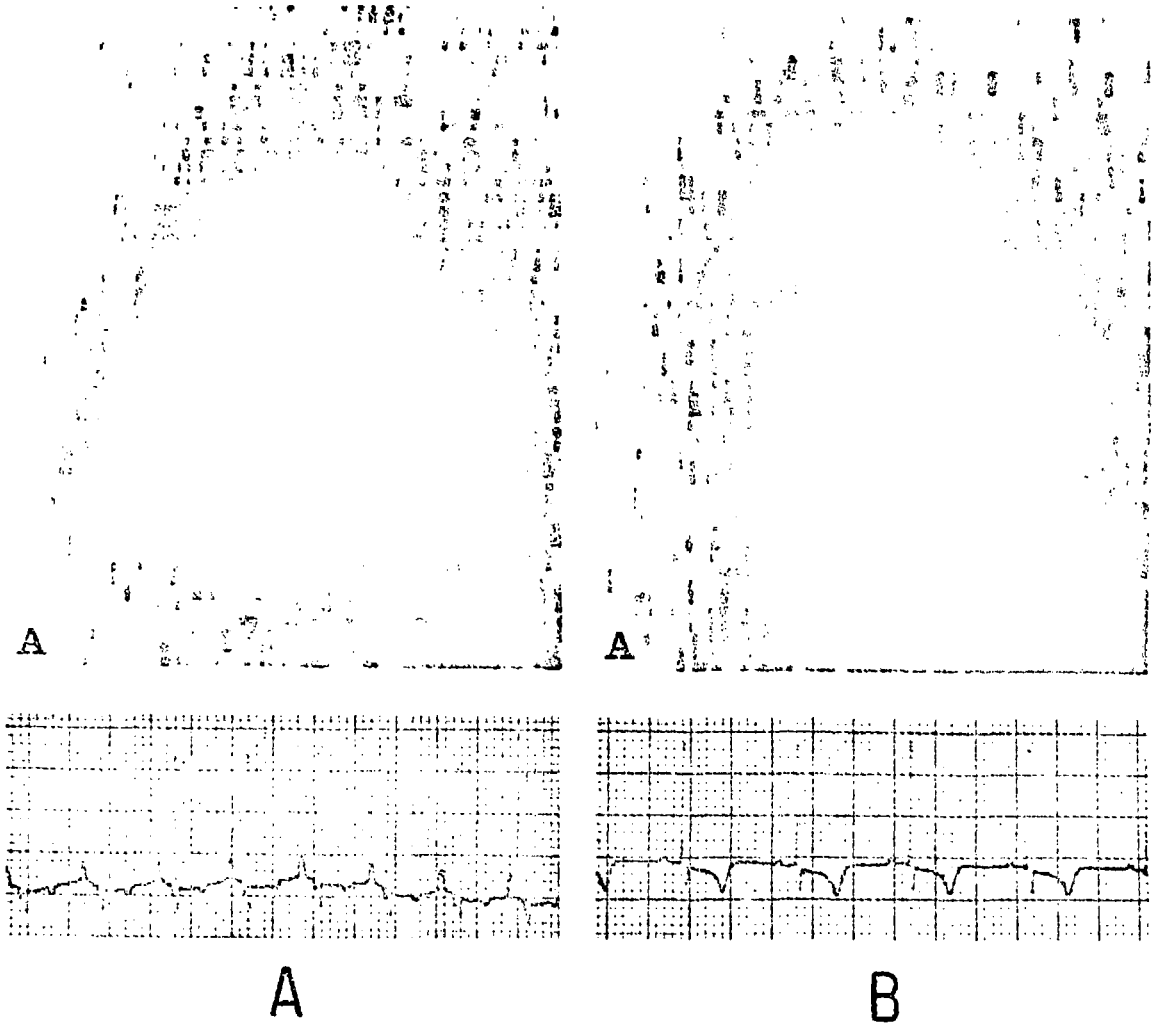

FIGURE 5.

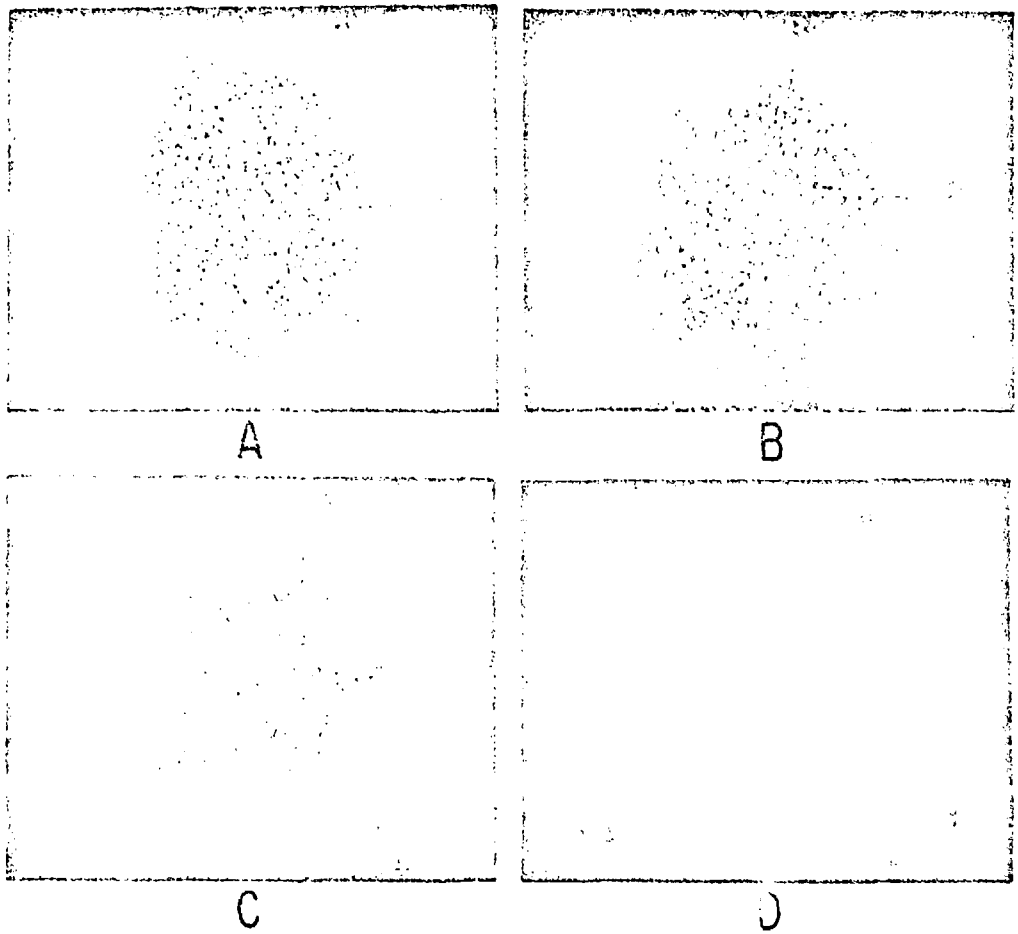

FIGURE 6.

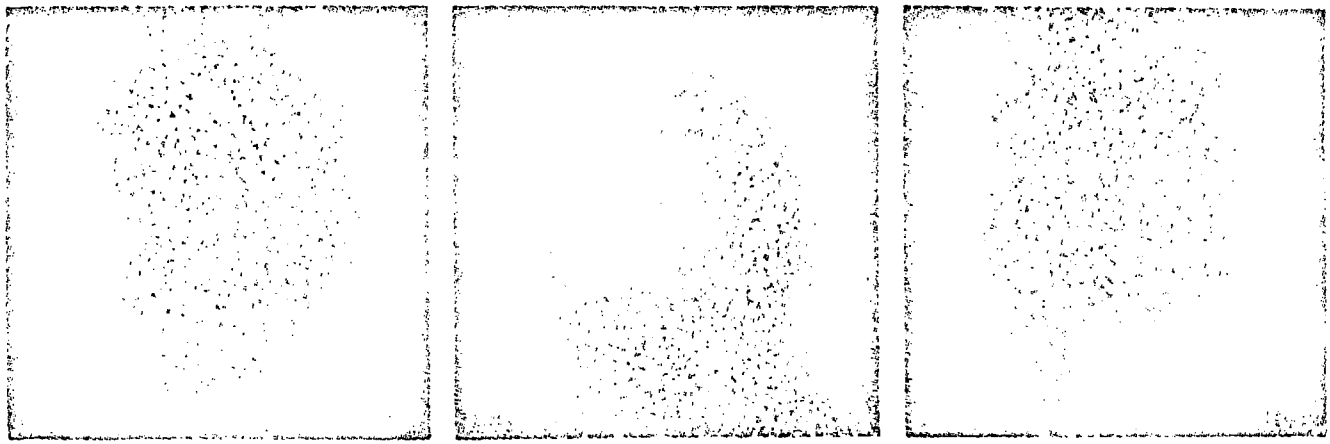

FIGURE 7.

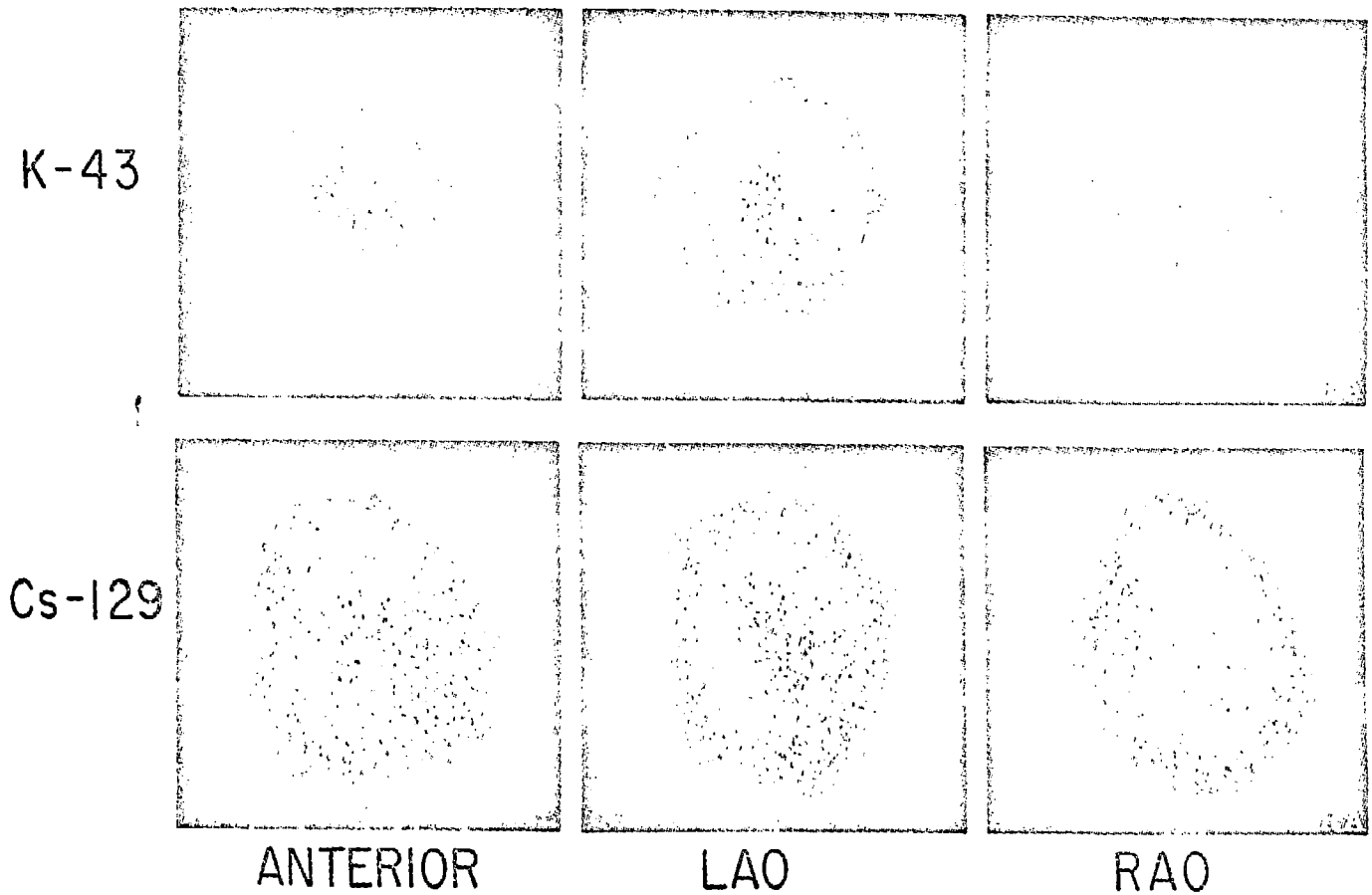

FIGURE 8.

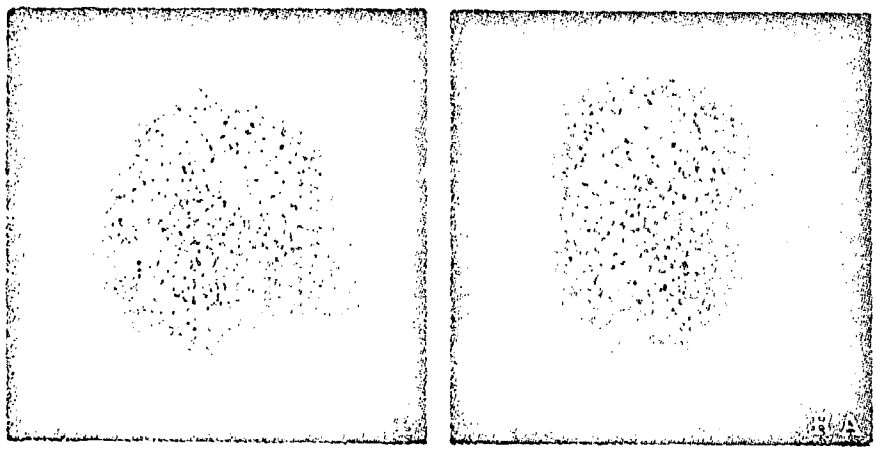

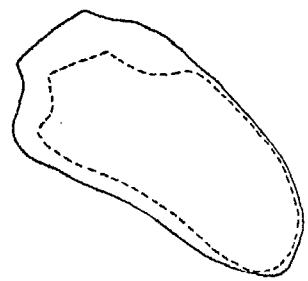

FIGURE 9.